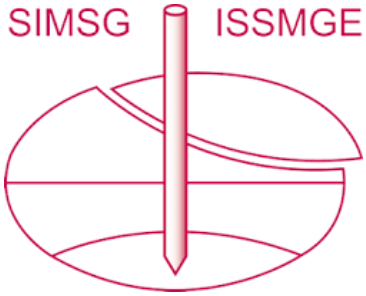
INTERNATIONAL SOCIETY FOR
SOIL MECHANICS AND
GEOTECHNICAL ENGINEERING




*This paper was downloaded from the Online Library of the International Society for Soil Mechanics and Geotechnical Engineering (ISSMGE). The library is available here:*

*https://www.issmge.org/publications/online-library*

*This is an open-access database that archives thousands of papers published under the Auspices of the ISSMGE and maintained by the Innovation and Development Committee of ISSMGE.*

*The paper was published in the proceedings of the 6th International Conference on Geotechnical and Geophysical Site Characterization and was edited by Tamás Huszák, András Mahler and Edina Koch. The conference was originally scheduled to be held in Budapest, Hungary in 2020, but due to the COVID-19 pandemic, it was held online from September 26th to September 29th 2021.*

# Dynamic Modulus, Young's Modulus and Damping Ratio Measurements of Fly Ash from Fixed-Free Resonant Column Apparatus

Archana Mallick
*Indian Institute of Technology, Kharagpur, India, archana.civil2011@gmail.com*

Dilip Kumar Baidya
*Indian Institute of Technology, Kharagpur, India, baidya@civil.iitkgp.ac.in*

**ABSTRACT:** Large quantities of fly ash are being generated at a global level by thermal power plants. For the bulk utilization of fly ash in the field of geotechnical engineering, a relatively good understanding of the characteristics of fly ashes, their response and engineering behavior in the field is essential. The utilization of fly ash in embankments of earthquake-prone regions requires a thorough analysis and knowledge of its dynamic properties. In the present study fixed-free type of resonant column tests have been carried out on fly ash to analyse the influence of various factors on the dynamic shear modulus (G), Young's modulus (E) and Damping ratio (D) with the shear strain in the range of 0.0005-0.05%. The specimens are subjected to varying confining pressures of 50 kPa to 400 kPa. The dynamic modulus, Young's modulus and damping ratio are found to be dependent upon the confining pressure and shear strain.

**Keywords:** shear modulus; young's modulus; damping ratio; fly ash

## 1. Introduction

Power generation in India is primarily coal/lignite based with about 80% of electricity generation obtained from coal based thermal power stations. India has coal reserves of 319.04 billion tonnes and 167 nos. of thermal power stations. Indian coal has high ash content (30-45%) which results in fly ash generation of large quantity. In the year 2017-18, the amount of fly ash generated was estimated to be 196.44 million tons. Fly ash disposal is a matter of concern since it requires large area for its safe disposal without causing pollution of air and water. Therefore, it is imperative to find out alternative uses for bulk utilization of fly ash without causing adverse effects on environment.

Numerous studies are available on the behavior of fly ash as a construction material. Study on unprocessed, compacted fly ash as structural fill was carried out by Martin et al. [1]. Kaniraj and Gayathri [2] carried out tests to study permeability and consolidation characteristics of fly ash. Kim et al. [3] studied the use of fly ash and bottom ash mixture as construction material in highway embankments. Compaction characteristics study carried out by Prakash and Sridharan [4] suggest that compacted dry unit weights are insensitive to moisture content variation. Effect of addition of various additives such as lime kiln dust(Kang et al. [5]), cement, fiber (Kumar and Gupta [6]), spent coffee grounds (Arulrajah et al. [7]) have also been studied. Malik and Shah [8] conducted plate load tests on compacted fills of fly ash (*FA*), fly ash (*FA*)-waste sludge (*S*), fly ash (*FA*)-cement (*C*) and fly ash (*FA*)-cement (*C*)-waste sludge (*S*) to assess their bearing capacity. Keatts et al. [9] experimentally studied relationships between apparent contact angle, dry density, and water entry head for a Class-F coal fly ash and Ottawa sand. Das et al.[10] carried out experiments to study the effect of randomly distributed geofibers on the seepage velocity and piping resistance of fly ash. It was reported that introduction of fibers reduced the seepage velocity and increased the piping resistance of fly ash. Erdal [11] conducted tests to determine chemical composition, grain size distribution, consistency limits, and free swell tests of expansive soil-lime, expansive soil-fly ash and expansive soil-cement samples. Erdem et al. [12] investigated the resilient moduli and unconfined compressive strength of the organic soils modified by fly ash. Indraratna et al. [13] conducted tests on ASTM Class C fly ash and suggested its use as an effective fill for embankments. Lo and Wardani [14] conducted triaxial tests on cmented silts to determine the mechanical behavior and reported that cemented soils became more dilatant than parent soils.

Boominathan and Hari [15] conducted cyclic triaxial tests on fly ash samples reinforced with randomly distributed fiber and assessed liquefaction resistance of fly ash. Chattaraj and Sengupta [16] suggested correlations for predicting the value of maximum dynamic shear modulus ($G_{max}$) for the fly ash based on confining pressure and void ratio. Saride and Dutta [17] conducted fixed-free type resonant column tests for determination of dynamic properties of fly ash treated with and without expansive soils. Madhusudhan and Senetakis [18] carried out tests on Bangalore sand in flexural mode of vibration to determine elastic Young's modulus values and material damping. The review of literature indicates that very few studies are available on strain dependent dynamic properties of fly ash. For assessing suitability of fly ash as an embankment material, it is also necessary to consider the dynamic behaviour of fly ash in an earthquake prone region. Hence the focus of the present study is to assess the dynamic behaviour of fly ash in order to ensure its suitability as a geomaterial.

## 2. Experimental Procedures

The fly ash used in the present investigation is collected from Kolaghat thermal power station, West Bengal. The particle size distribution is shown in Fig.1. It is found that fly ash primarily consists of silt sized (about 75% by weight) particles. In Fig. 1 comparison of the particle size distribution of fly ashes collected from Parichha power plants, Panki power plants and Neyveli Lignite Corporation are also presented (Das and Yudhbir, 2005 [19]). It may be seen from the figure that the grain size curve of the present fly ash sample lies within Panki fly ash and Parichha fly ash.

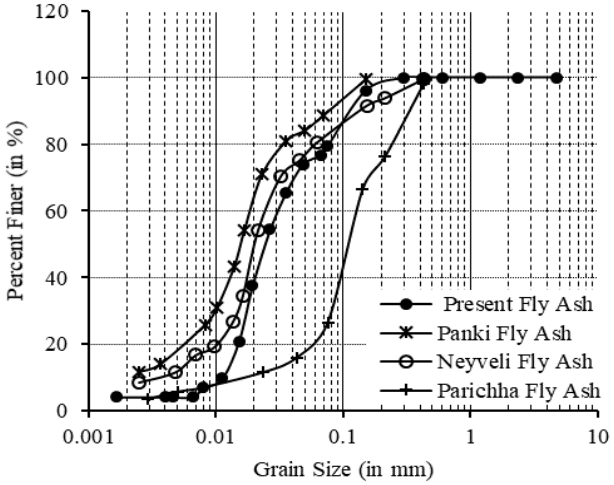



**Figure 1.** Particle size distribution curve for fly ash

Fig. 2 represents the compaction curve for the fly ash. It may be seen from the figure that moisture-density curve is relatively flat indicating that dry density does not change significantly with the variation of moisture content. Similar behavior has also been reported by Martin et al. [1] and Ghosh and Subbarao [20].

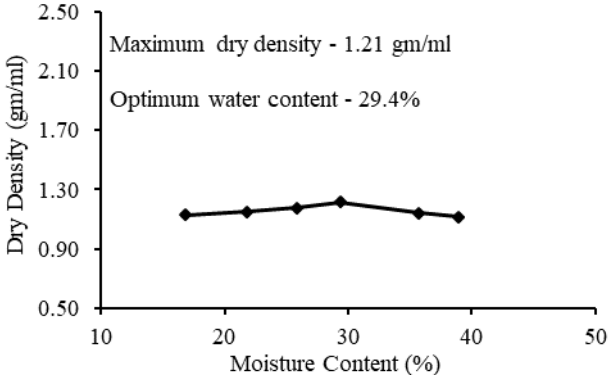



**Figure 2.** Compaction curve for fly ash

Table 1 and Table 2 present the chemical composition and geotechnical properties of fly ash, respectively.

**Table 1.** Chemical composition of fly ash

| Chemical Compound | Concentration (%) |
|---|---|
| $SiO_2$ | 59.021 |
| $Al_2O_3$ | 29.220 |
| $Fe_2O_3$ | 6.177 |
| CaO | 0.679 |
| MgO | 0.679 |
| Others | 4.224 |

**Table 2.** Geotechnical properties of fly ash

| Properties | Values |
|---|---|
| Specific Gravity | 2.15 |
| Effective Size, $D_{10}$ (mm) | 0.012 |
| $D_{30}$ (mm) | 0.018 |
| $D_{60}$ (mm) | 0.03 |
| Coefficient of Uniformity, $C_u$ | 2.5 |
| Coefficient of Curvature, $C_c$ | 0.9 |
| Maximum Dry Density (gm/ml) | 1.19 |
| Optimum Moisture Content (%) | 28.4 |

### 2.1. Preparation of samples

Fly ash samples are prepared by static compaction technique (in three layers). The test samples are 70 mm in diameter and 140 mm in length. Depending upon the density of the sample to be achieved, the required amounts of dry fly ash and water are taken. They are mixed thoroughly. The prepared mix is then poured into the mold in three layers. After pouring the first layer, static compaction is applied to achieve one-third height of the sample. The top of the surface is scarified before pouring the second layer in order to ensure proper bonding between consecutive layers. The process is repeated until full height of the sample is achieved. The sample is then extruded from the mold for testing.

## 3. Resonant Column Test

The tests are carried out in a fixed-free type resonant column device. Fig. 3 presents the resonant column apparatus. After placing specimen on the pedestal, the top-cap is positioned on the top of the specimen. Then the drive system, consisting of four magnets, is attached to the top-cap. It is ensured that each magnet within the coils is able to move freely. For the application of air pressure, the confining chamber is placed on the resonant column unit. The resonant column test is performed by applying a sinusoidal excitation through a torque producing system. During torsional test, four pairs of coils are connected in a series to produce a net torque and during flexural test, only two magnets are used to apply a horizontal force to the specimen. After the application of air pressure, a small amount of voltage is applied to produce torque on the specimen through the coils at a frequency range of 30-200 Hz with an increment of 5 Hz. This process is called Broad Sweeping or Coarse sweeping and it roughly determines the natural frequency of the sample. Once the broad sweep is completed, fine sweeping is conducted at a frequency range of ±5 Hz on either side of the roughly estimated natural frequency, with an increment of 0.1 Hz, to detemine the natural frequency accurately. The voltage in the coils is increased gradually and the above process is repeated at each increment until the shear strain exceeds 0.01%. Confining pressures of 50 kPa, 100 kPa, 200 kPa, and 400 kPa are applied with the value of shear strain varying in the range of $0.0005\% \leq \gamma \leq 0.01\%$. Both torsional and flexural tests are conducted on fly ash samples prepared at 70% and 100% relative densities.



**Figure 3.** Resonant Column Unit

## 3.1. Torsional Test

The shear wave velocity is calculated from the following Eq. (1),

$$V_s = \frac{2\pi f l}{\beta} \tag{1}$$

where,

$V_s$ = shear wave velocity (in m/s);

$f$ = natural frequency of sample found from resonant column test (in Hz); and

$l$ = length of sample (in m).

$\beta$ is found from the basic equation of fixed-free resonant column given by Eq. (2) given below,

$$\frac{I}{I_0} = \beta \tan \beta \tag{2}$$

where,

$I$ = mass polar moment of inertia of cylindrical soil sample = $md^2/8$ (mass is in kg and diameter is in m); and

$I_0$ = mass polar moment of inertia of drive system (found out experimentally from calibration of the system).

Shear Modulus ($G$) is then found out using the following relationship,

$$G = \rho V_s^2 \tag{3}$$

where $\rho$ = density of soil specimen.

The viscous damping ratio ($D$) is measured from the shape of the free vibration decay curve. The logarithmic decrement ($\delta$) is calculated by taking logarithm of the ratio of amplitudes of successive cycles. Then damping ratio is calculated using equation (4) given below:

$$D = \sqrt{\frac{\delta^2}{4\pi^2+\delta^2}} \tag{4}$$

## 3.2. Flexural Test

The specimen and drive mechanism are idealized as an elastic column with a lumped mass at its free end. Applying Rayleigh's Energy method i.e.no energy is lost in the system and total energy is constant. From Cascante [21] the following equation is obtained using Rayleigh's method and considering N distributed masses $m_i$.

$$\omega_f^2 = \frac{3EI_b}{L^3\left[\frac{33}{140}m_T+\sum_{i=1}^{N} m_i.h(h0_i,h1_i)\right]} \tag{5}$$

where

$$h(h0_i,h1_i) = \left[1+3\frac{(h0_i+h1_i)}{2L}+\frac{3}{4}\left(\frac{h0_i^2+h0_ih1_i+h1_i^2}{L^2}\right)\right]$$

$h0_i$, $h1_i$=heights at bottom and top, respectively of mass $i$ as measured from the top of soil specimen

$E$=Young's modulus of specimen

$I_b$=area moment of inertia of specimen

$m_T$=mass of the specimen

Eq. (5) can also be expressed in terms of center of gravity $y_{ci}$ and area moment of inertia with respect to the center of gravity $I_{yi}$ of each mass $m_i$.

$$\omega_f^2 = \frac{3EI_b}{L^3\left[\frac{33}{140}m_T+\sum_{i=1}^{N} m_i+\frac{3m_iy_{ci}}{L}+\frac{9(I_{yi}+m_iy_{ci})}{4L^2}\right]} \tag{6}$$

Similarly Eq. (6) can also be represented as,

$$h\left(y_{ci}, I_{yi}\right) = 1+\frac{3y_{ci}}{L}+\frac{9}{4L^2}\left[\frac{I_{yi}}{m_i}+y_{ci}^2\right] \tag{7}$$

Young's modulus, $E_{flex}$ is calculated based on the geometric properties of specimen and apparatus, and resonant frequency of flexural vibration.

The longitudinal wave velocity, $V_{LF}$ in a rod can be calculated from $E_{flex}$ and density of the specimen, $\rho$:

$$V_{LF} = \sqrt{\left(\frac{E_{flex}}{\rho}\right)} \tag{8}$$

## 4. Results and Discussion

### 4.1.1. Effect of confining pressure on Shear modulus (G)

Variation of shear modulus with torsional shear strain, for fly ash at 70% and 100% relative density (RD), is shown in Fig. 4. It may be seen from the figure that at constant confining pressure (CP), value of shear modulus degrades with strain. The reference strain for fly ash is found to be 0.001% based on the experimental data. The tests are terminated when a strain of 0.01% is achieved. The interrelation between normalized shear modulus ($G/G_{max}$) degradation and shear strain is shown in Fig. 5 at different confining pressures. It may be seen that at constant confining pressure, shear modulus degrades with shear strain. The relationship between degradation of shear modulus and confining pressure is found to be inversely proportional. At 50 kPa confining pressure, the shear modulus degrades by 24%. However, at 400 kPa confining pressure the degradation is measured to be 9%.

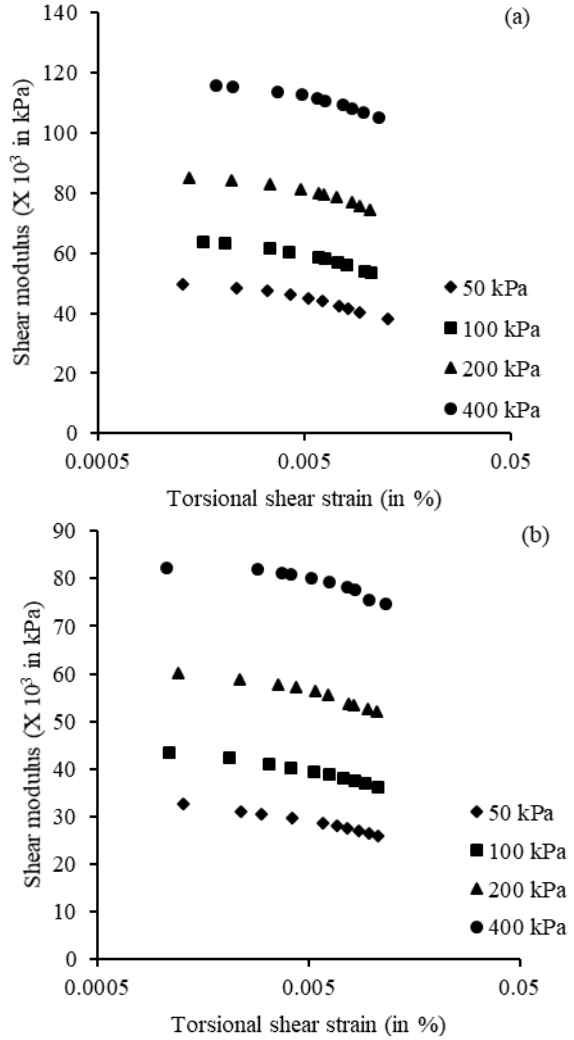



**Figure 4.** Variation of shear modulus with torsional shear strain for fly ash at (a) 100% relative density and (b) 70% relative density

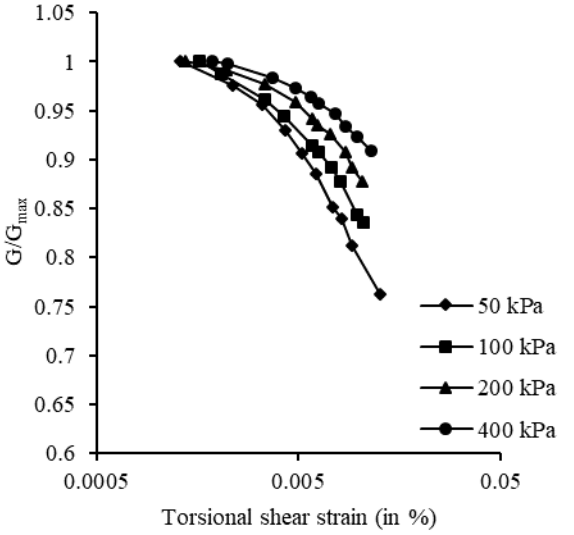



**Figure 5.** Variation of shear modulus degradation with torsional shear strain for fly ash at 100% relative density

### 4.1.2. Effect of confining pressure on damping ratio (D)

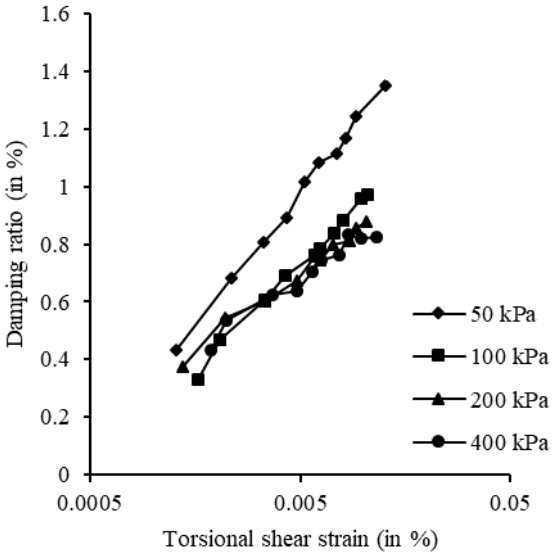



**Figure 6.** Variation of damping ratio with torsional shear strain for fly ash at 100% relative density

Figure 6 shows the effect of confining pressure on damping ratio of fly ash at relative density of 100%. It may be seen that at constant confining pressure, damping ratio increases with strain amplitude. The relationship between confining pressure and damping ratio is found to be inversely proportional. Similar trend is also reported in literature [16].

### 4.1.3. Effect of void ratio (e) on shear modulus (G)

Figure 7 shows the interrelation between modulus degradation with strain.

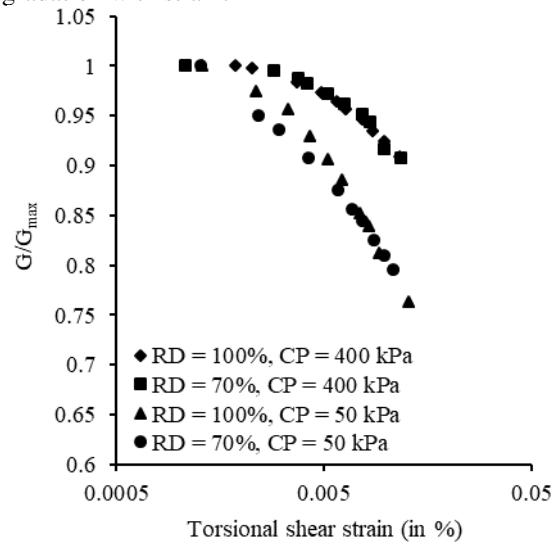



**Figure 7.** Variation of shear modulus degradation with torsional shear strain for fly ash at constant confining pressure

It may be seen from the figure that shear modulus degradation is dependent upon shear strain at a given value of confining pressure and void ratio. The effect of void ratio on the variation is found to be negligible.

### 4.1.4. Effect of void ratio on torsional damping ratio (D)

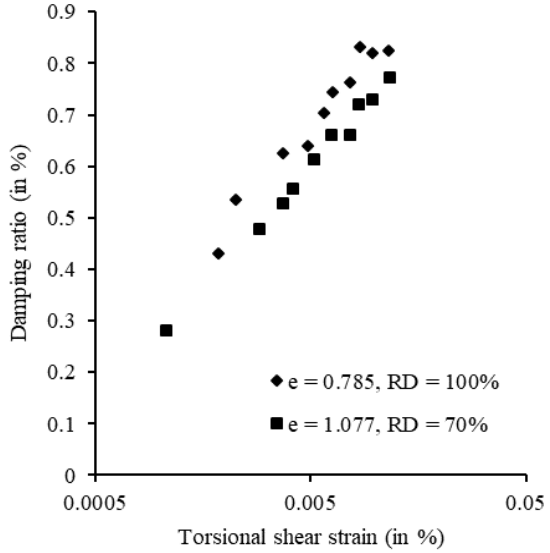



**Figure 8.** Variation of damping ratio with torsional shear strain for fly ash at 400 kPa confining pressure

Figure 8 shows the relationship between damping ratio and torsional shear strain. It is observed that the values of damping are quite close to each other for two different relative densities of fly ash. It implies that damping of fly ash is greatly influenced by shear strain and is not significantly influenced by the void ratio (relative density). Similar trend is observed at all confining pressures.

### 4.1.5. Effect of confining pressure on maximum shear modulus ($G_{max}$)

Figure 9 shows the effect of confining pressure on maximum dynamic shear modulus at different relative densities.

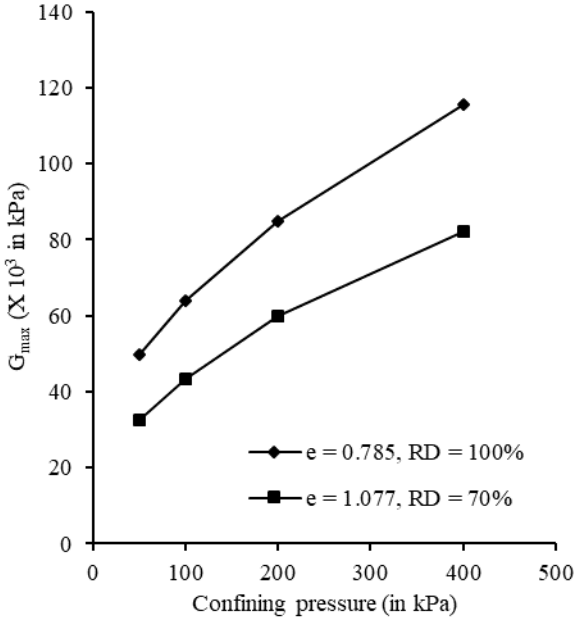



**Figure 9.** Variation of maximum shear modulus with confining pressure at different relative densities

It may be seen from the figure that $G_{max}$ increases with confining pressure at constant relative density. This behavior may be attributed to the fact that with increase in confining pressure, stiffness of fly ash also increases. The increase in the values of $G_{max}$ are found to be 132% and 151% for fly ash at void ratio of 0.785 and 1.077 respectively.

### 4.1.6. Effect of confining pressure on Young's modulus (E)

Figure 10 shows the variation of Young's Modulus with flexural strain at different confining pressures.

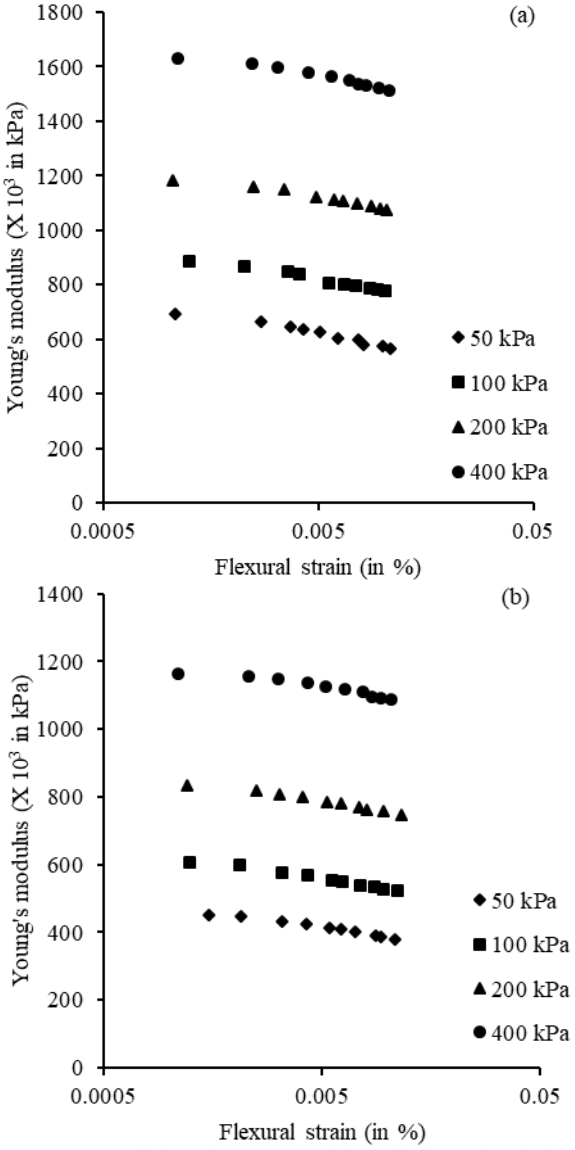



**Figure 10.** Variation of Young's modulus with flexural strain for fly ash at (a) 100% relative density and (b) 70% relative density

It may be seen that $E_{flex}$ increases with increase in confining pressure. This behavior is similar to the variation of shear modulus with confining pressure.

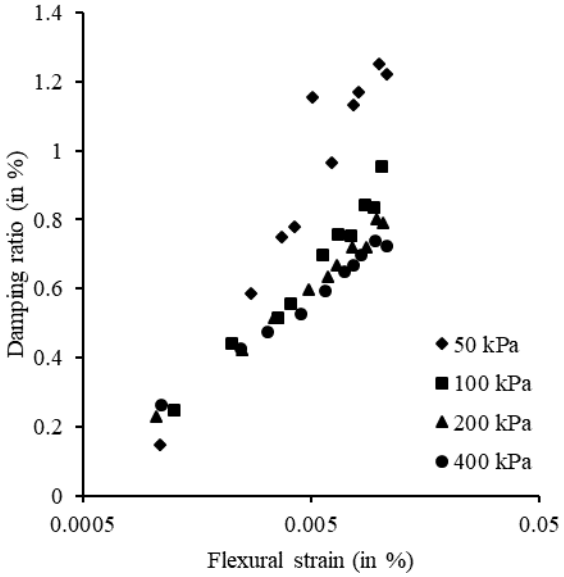



**Figure 11.** Variation of damping ratio with flexural strain for fly ash at 100% relative density

Figure 11 shows the variation of damping ratio with flexural strain. It may be seen that the trend is similar to the behavior of damping ratio with torsional shear strain. Damping ratio is found to decrease with increase in confining pressure at constant relative density. At 70% relative density similar behavior is also observed.

### 4.1.7. Effect of void ratio on flexural damping ratio ($D_f$)

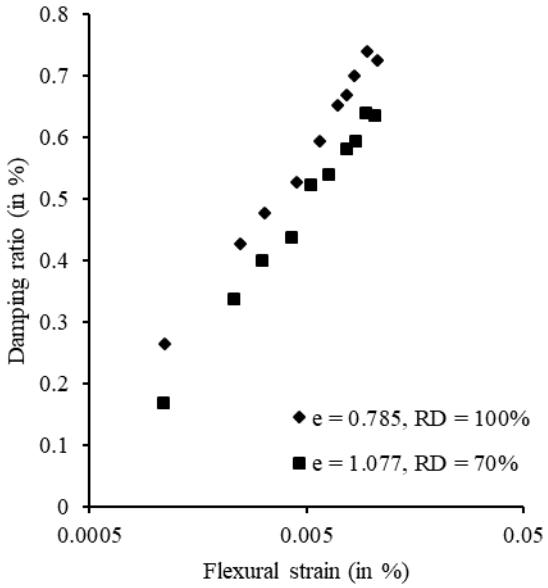



**Figure 12.** Variation of damping ratio with flexural strain for fly ash for different relative densities at 400 kPa confining pressure

Figure 12 shows the effect of void ratio on flexural damping at 70% and 100% relative densities. It may be seen from the figure that the trend is similar to the behavior of torsional damping as shown in Fig. 8. The damping ratio does not greatly depend upon the void ratio but is dependent upon strain amplitude. Torsional damping ($D$) is found to be higher in magnitude than the flexural damping ($D_f$) at all confining pressures. At relative density of 100% and lower confining pressure of 50 kPa, the ratio ($D_f/D$) is found to fall in the range of 0.3-1.13. At 400 kPa confining pressure, the value lies in the range of 0.6-0.89.

Figure 13 shows the effect of confining pressure on Young's modulus at 70% and 100% relative densities.

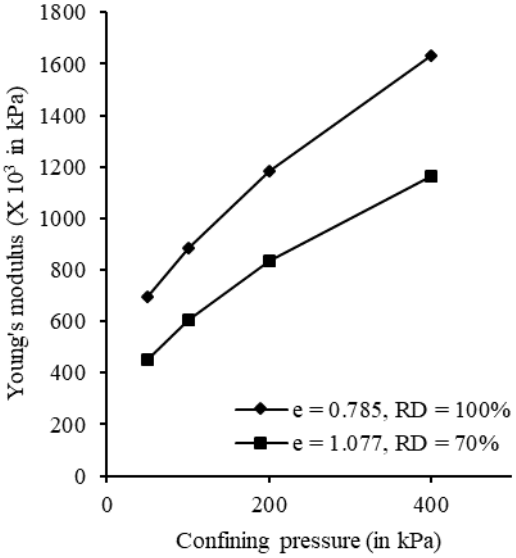
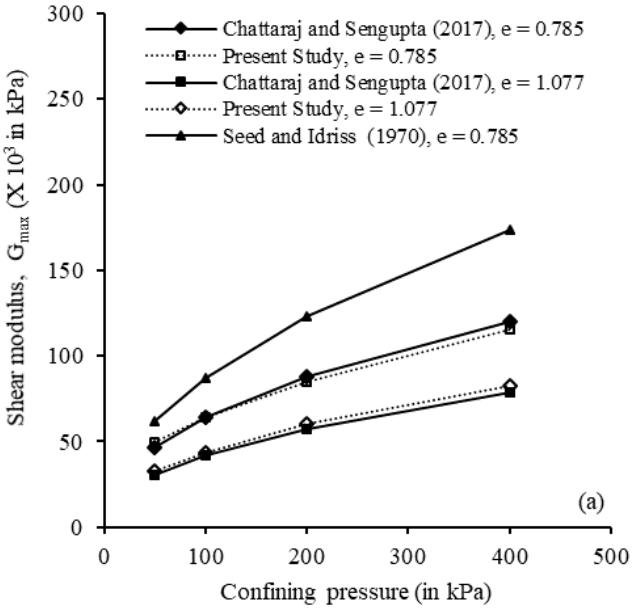



**Figure 13.** Variation of Young's modulus with confining pressure at different relative densities

It may be seen from the figure that Young's modulus increases with increase in confining pressure at constant relative density. Similar behavior is also observed in Fig. 9 for variation of $G_{max}$. The increase in the values of $E_{flex}$ are found to be 135% and 157% for fly ash at void ratio of 0.785 and 1.077 respectively.

### 4.1.8. Comparison of $G_{max}$ and torsional damping ratio (D) with other studies

The values of $G_{max}$ and torsional damping ratio ($D$) obtained from the experimental results are compared with the empirical relations suggested for fly ash by Chattaraj and Sengupta [16], and for sand by Seed and Idriss [22]. Equation (9) and Eq. (10) represent the relations for estimation of $G_{max}$ and damping ratio of fly ash, respectively. Equation (11) represents the relation for estimation of maximum shear modulus of sand. Figures 14 (a) and 14 (b) show the comparison of values of $G_{max}$ and torsional damping ratio. In Eq. (11), $K_{2,max}$ is determined from the void ratio or relative density of sand. It may be seen from the Fig. 14 (a) that the value of $G_{max}$ obtained from the Eq. (9) and the experimental data are in good agreement. The data obtained from Equation (11) are higher than the experimental $G_{max}$ values of fly ash. It may be attributed to the fact that stiffness of sand is higher than that of fly ash. From Fig. 14 (b) it may be observed that the damping values of fly ash of different relative densities are lying close to the values obtained from Eq. (10) at 50 kPa. It is also observed that damping ratio values are more dependent upon shear strain amplitude than relative density or void ratio as observed in Fig. 8.



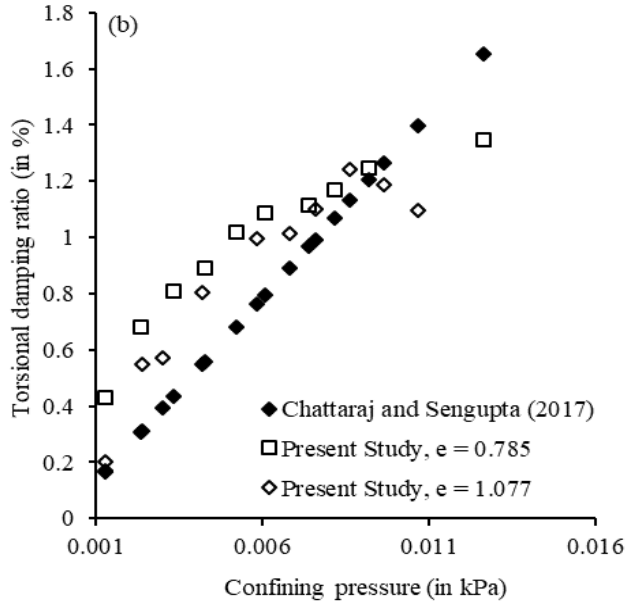




**Figure 14.** Comparison of observed values with predicted values of (a) $G_{max}$ at different confining pressures and (b) torsional damping ratio, $D$ at 50 kPa

$$G_{max} = \frac{463.98\times(P_a)^{0.545}\times(\sigma_0)^{0.455}}{(0.3+0.7e^2)} \quad (9)$$

$$D_s = 115.65\left(\frac{\sigma_0}{P_a}\right)^{-0.175}(\gamma) \quad (10)$$

$$G_{max} = 1000\,K_{2,max}\,(\sigma'_m)^{0.5} \quad (11)$$

## 5. Conclusions

The dynamic behavior of fly ash has been reviewed in the present paper. It is observed that value of dynamic shear and Young's modulus degrade with increase in the value of strain amplitude. It is observed that at 50 kPa confining pressure, the shear modulus degrades by 24% and at 400 kPa confining pressure the degradation is measured to be 9% with strain amplitude in the range of 0.001%-0.01%. This decrease in the rate of degradation may be attributed to the fact that increase in confining pressure increases the stiffness of fly ash. It is observed that at constant confining pressure rate of shear modulus degradation does not depend significantly on relative density. It is observed that torsional damping ratio and flexural damping ratio are very much influenced by confining pressure and strain amplitude. Young's modulus is found to increase by 135% and 157% at void ratio of 0.785 and 1.077 respectively. Torsional damping of fly ash is found be higher than flexural damping of fly ash. The experimentally obtained data of damping ratio (torsional) and dynamic shear modulus are compared with data obtained from the relations suggested by Chattaraj and Sengupta [16], and Seed and Idriss [22]. It is observed that $G_{max}$ values of sand are higher than the $G_{max}$ values of fly ash. The experimental data obtained are in agreement with the data obtained from the relations suggested by Chattaraj and Sengupta [16].

## References


[1] Martin, Joseph P., Collins, Robert A., Browning, John S., Biehl, Francis J. "Properties and use of fly ashes for embankments", Journal of Energy Engineering, 116(2), pp. 71–86, 1990. https://doi.org/10.1061/(ASCE)0733-9402(1990)116:2(71)

[2] Kaniraj, Shenbaga R., Gayathri, V. "Permeability and consolidation characteristics of compacted fly ash", Journal of Energy Engineering, 130(1), pp. 18–43, 2004. https://doi.org/10.1061/(ASCE)0733-9402(2004)130:1(18)

[3] Kim, B., Prezzi, M., Salgado, R. "Geotechnical properties of fly and bottom ash mixtures for use in highway embankments" Journal of Geotechnical and Geoenvironmental Engineering, 131(7), pp. 914–924, 2005. https://doi.org/10.1061/(ASCE)1090-0241(2005)131:7(914)

[4] Prakash, K., Sridharan, A. "Beneficial properties of coal ashes and effective solid waste management", Practice Periodical of Hazardous, Toxic, and Radioactive Waste Management, 13(4), pp. 239–248, 2009. https://doi.org/10.1061/(ASCE)HZ.1944-8376.0000014

[5] Kang, X., Kang, G., Chang, K., Ge, L. "Chemically stabilized soft clays for road-base construction", Journal of Materials in Civil Engineering, 27(7), 2015. https://doi.org/10.1061/(ASCE)MT.1943-5533.0001156

[6] Kumar, A., Gupta, D. "Behavior of cement-stabilized fiber-reinforced pond ash, rice husk ash soil-mixtures", Geotextiles and Geomembranes 44(3), pp. 466–474, 2016. https://doi.org/10.1016/j.geotexmem.2015.07.010

[7] Arulrajah, A., Kua, T., Phetchuay, C., Horpibulsuk, S., Mahghoolpilehrood, F., Disfani, M. "Spent coffee grounds-fly ash geopolymer used as an embankment structural fill material", Journal of Materials in Civil Engineering, 28(5), 2016. https://doi.org/10.1061/(ASCE)MT.1943-5533.0001496

[8] Malik, S.A., Shah, S.S. "Load settlement behaviour of fly ah mixed with waste sludge and cement", Geotechnical and Geological Engineering, 34(1), pp. 37–58, 2016. https://doi.org/10.1007/s10706-015-9927-z

[9] Keatts, Matthew I., Daniels, John L., Langley, William G., Pando, Miguel A., Ogunro, Vincent O. "Apparent contact angle and water entry head measurements for organo-silane modified sand and coal fly ash", Journal of Geotechnical and Geoenvironmental Engineering, 144(6), 2018. https://doi.org/10.1061/(ASCE)GT.1943-5606.0001887

[10] Das, A., Jayashree, Ch, Viswanadham, B.V.S. "Effect of randomly distributed geofibers on the piping behaviour of embankments constructed with fly ash as a fill material",Geotextiles and Geomembranes, 27(5), pp. 341–349, 2009. https://doi.org/10.1016/j.geotexmem.2009.02.004

[11] Erdal, C. "Use of Class C fly ashes for the stabilization of an expansive soil",Journal of Geotechnical and Geoenvironmental Engineering, 127(7), pp. 568–573, 2001. https://doi.org/10.1061/(ASCE)1090-0241(2001)127:7(568)
[12] Erdem, T.O., Edil, T.B., Benson, C.H., Aydilek, A.H. "Stabilization of organic soils with fly ash", Journal of Geotechnical and Geoenvironmental Engineering, 137(9), pp. 819–833, 2011. https://doi.org/10.1061/(ASCE)GT.1943-5606.0000502
[13] Indraratna, B., Nutalaya, P., Koo, K.S., Kuganenthira, N. "Engineering behaviour of a low carbon, pozzolanic fly ash and its potential as a construction fill", Canadian Geotechnical Journal, 28(4), pp. 542–555, 1991. https://doi.org/10.1139/t91-070
[14] Lo, S. R.,Wardani, S. P. R. "Strength and dilatancy of a silt stabilized by a cement and fly ash mixture", Canadian Geotechnical Journal, 39(1), pp. 77–89, 2002. https://doi.org/10.1139/t01-062
[15] Boominathan, A., Hari, S. "Liquefaction strength of fly ash reinforced with randomly distributed fibers", Soil Dynamics and Earthquake Engineering, 22, pp. 1027–1033, 2002. https://doi.org/10.1016/S0267-7261(02)00127-6
[16] Chattaraj, R., Sengupta, A. "Dynamic properties of fly ash", Journal of Materials in Civil Engineering, 29(1), 2017. https://doi.org/10.1061/(ASCE)MT.1943-5533.0001712
[17] Saride, S., Tanu Dutta, T. "Effect of fly-ash stabilization on stiffness modulus degradation of expansive clays", Journal of Materials in Civil Engineering, 28(12), 2016. doi: https://doi.org/10.1061/(ASCE)MT.1943-5533.0001678
[18] Madhusudhan, B.N., Senetakis, K. "Evaluating use of resonant column in flexural mode for dynamic characterization of Bangalore sand", Soils and Foundations, 56(3), pp. 574–580, 2016. https://doi.org/10.1016/j.sandf.2016.04.021
[19] Das, S.K., Yudhbir. "Geotechnical Characterization of Some Indian Fly Ashes", Journal of Materials in Civil Engineering, 17(5), 2005. https://doi.org/10.1061/(ASCE)0899-1561(2005)17:5(544)
[20] Ghosh, A., Subbarao, C. "Strength characteristic of class F fly ash modified with lime and gypsum", Journal of Geotechnical and Geoenvironmental Engineering, 133(7), pp. 757–766, 2007. https://doi.org/10.1061/(ASCE)1090-0241(2007)133:7(757)
[21] Cascante, G., Santamarina, C., Yassir, N. "Flexural excitation in a standard torsional-resonant column device", Canadian Geotechnical Journal, 35, 478-490 (2007). https://doi.org/10.1139/t98-012
[22] Seed, H.B., Idriss, I.M. "Soil Moduli and damping factors for dynamic response analyses", Earthquake Engineering Research Center, University of California, Berkeley, United States, Rep. EERC 70-10, 1970.